The Bell System Technical Journal
Vol. 54, No. 2, February 1975
Printed in U.S.A.

Optical-Fiber Packaging and Its Influence on Fiber Straightness and Loss

By D. GLOGE

(Manuscript received August 5, 1974)

Glass fibers are in general not thick enough to withstand external forces on their own without suffering axial distortion, mode coupling, and loss. Thus, plastic jackets must be carefully designed to provide effective protection. We evaluate jacket designs ranging from the merc use of soft materials to the application of multiple plastic coatings and graphite reinforcement. We compute the distortion loss as a function of dimensional variations and of lateral forces considered typical for cable packaging. The protective quality of a jacket is found to depend on a combination of stiffness and compressibility and on the fiber characteristics.

I. INTRODUCTION

Surprisingly small external forces can cause lateral deformations, mode coupling, and optical loss in clad fibers. For example, minute irregularities in the machined surface of a metal drum suffice to cause substantial loss in fibers wound on this drum with only a few grams of tension.[1] (An interesting and valuable study of this subject is described by W. B. Gardner.[2]) The pressure exerted on the individual fiber in a cable will almost certainly be considerably stronger and less uniform. The concern with this effect has heightened recently with the notion that lowest loss values are measured almost invariably in connection with extremely small mode coupling and after carefully eliminating external forces on the fiber.[3–5] Maintaining these loss values in a cable may require better fiber and, more importantly, effective jackets designed to optimally shield against external forces. This paper addresses the latter problem.

After gaining some insight into fiber deformation, we compute the excess transmission loss[6] resulting from statistical surface variations and lateral pressures affecting the fiber. The reader who is mainly interested in the results of this theory may wish to turn to Sections V or VI immediately, where practical examples and suggestions for an improved jacket design are discussed. We show that some care in this

respect substantially reduces the excess loss resulting from fiber distortion by outside forces.

II. ELASTIC DEFORMATIONS

We begin with the simple model of a fiber pressed against an elastic plane surface that is slightly rough (Fig. 1). The pressure from above is uniform, but as a result of the roughness, the contact forces between the fiber and the surface are not uniform along the fiber. Thus, the fiber bends slightly yielding to a force $f(z)$ per unit length.

According to the theory of the thin elastic beam, the lateral displacement $x(z)$ of the fiber axis is related to $f(z)$ by

$$\frac{d^4x}{dz^4} = \frac{f}{H}, \tag{1}$$

where

$$H = EI \tag{2}$$

is the flexural rigidity or stiffness; E is Young's modulus and I the moment of inertia. For the circular cross section of the fiber,

$$I = \frac{\pi}{4} a_1^4, \tag{3}$$

where a_1 is the radius of the fiber.

The force $f(z)$ not only causes a bending action, but also a deformation $u(z)$ of the surface. Provided that $f(z)$ does not change too drastically along z, $u(z)$ is a linear function of the force applied.[7] We introduce a factor of proportionality D, which we call the lateral rigidity, so that

$$u(z) = \frac{f(z)}{D}. \tag{4}$$

For the case of the elastic surface of Fig. 1, D is simply Young's modulus of the compressed surface material (we ignore a coefficient close to unity). To simplify the following steps, we assume temporarily that the surface is sufficiently compressible to conform to the fiber, producing a continuous line of contact. This imposes the relation

$$x + u - u_0 = v, \tag{5}$$

where $u_0 = \langle u \rangle$ is the average of $u(z)$ along z (see Fig. 1). Equations (1), (4), and (5) combined yield the differential equation

$$\frac{H}{D}\frac{d^4x}{dz^4} + x = v. \tag{6}$$

We now introduce the Fourier transforms $X(K)$ and $V(K)$ of $x(z)$ and $v(z)$. They are functions of a wave number K or a wavelength Λ

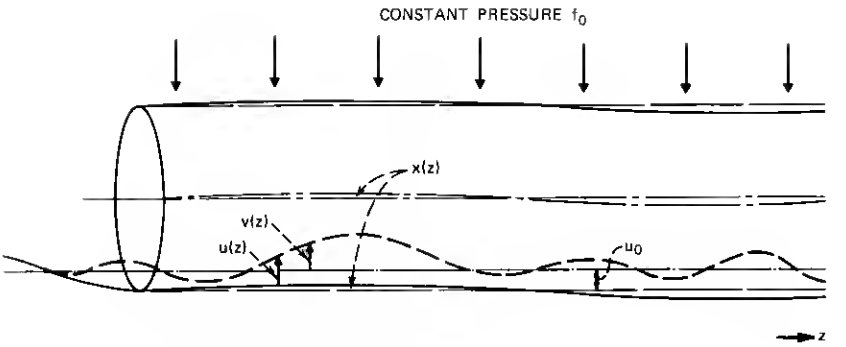

Fig. 1—Sketch of a fiber pressed against a rough surface by a uniform force (vertical dimensions strongly magnified).

related to K hy

$$K = 2\pi/\Lambda. \tag{7}$$

In the Fourier domain, eq. (6) takes the form

$$X = \frac{V}{1 + K^4H/D}. \tag{8}$$

According to (8), the effect each Fourier component V has on the fiber displacement depends strongly on the wavelength of that component. Periodic disturhances having a wavelength smaller than

$$R = 2\pi(H/D)^{\frac{1}{4}} \tag{9}$$

hardly affect the fiher, while those with longer wavelengths than (9) are almost fully reproduced. The length R is called the retention length in the following, hecause it qualifies the usefulness of a given fiher package to keep the fiher in its natural straight condition.

III. INCOMPLETE CONTACT

Assume $v(z)$ to be a random variahle measured from a suitahle reference plane so that its mean is zero as in Fig. 1. Characterize the random process of which $v(z)$ is a sample function hy the (power) spectral density $P_v(K)$. If a complete line of contact exists hetween the fiher and the surface, we can apply (8) to P_v so that the spectral density P_x of x hecomes $P_x = P_v(1 + HK^4/D)^{-2}$.

If the contact is not complete, we have the situation of Fig. 2. Figure 2a depicts the case in which the fiher is very stiff and stays almost straight, while only the highest elevations of the rough surface are compressed. We assume a mean spacing t hetween the fiher periph-

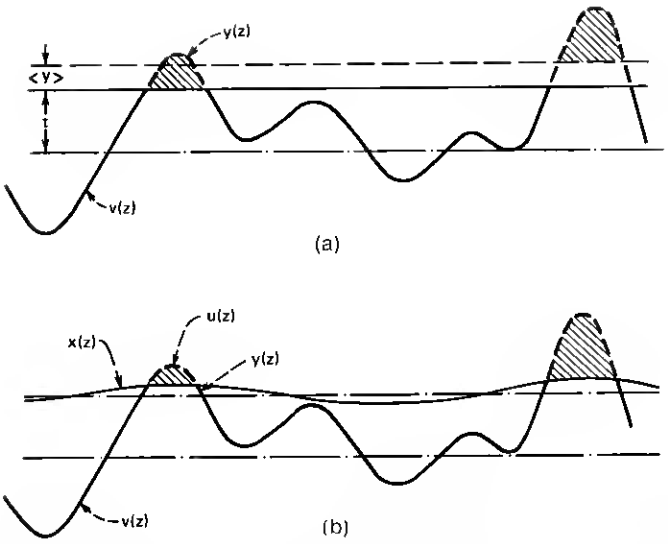

Fig. 2—Sketch of a fiber in incomplete contact with a rough surface. (a) The fiber is very stiff. (b) The fiber yields to bending. Cross-hatched areas indicate surface deformation (vertical dimensions strongly magnified).

ery and the surface. In this case the function causing the deformation is

$$y(z) = \begin{cases} v(z) - t & \text{for } v \geqq t \\ 0 & \text{for } v < t \end{cases} \tag{10}$$

rather than $v(z)$ itself. To obtain an approximate characterization of the random function y, we assume that $v(z)$ obeys a gaussian random process with standard deviation σ. The first two moments of y are, with this assumption,

$$\langle y \rangle = (2\pi)^{-\frac{1}{2}}\sigma^{-1} \int_t^\infty (v - t)e^{-v^2/2\sigma^2}dv \tag{11}$$

and

$$\langle y^2 \rangle = (2\pi)^{-\frac{1}{2}}\sigma^{-1} \int_t^\infty (v - t)^2 e^{-v^2/2\sigma^2}dv. \tag{12}$$

The variance of y is

$$s^2 = \langle y^2 \rangle - \langle y \rangle^2. \tag{13}$$

If one relates the spectral density P_y of $y - \langle y \rangle$ to that of v (for example, with the help of the Price method[7]), one finds the functional shape of both spectra to differ little for most cases of interest, so that the relation

$$\frac{P_y(K)}{P_v(K)} \approx \frac{s^2}{\sigma^2} \tag{14}$$

seems to be a useful approximation for all K. As y takes the place of v in (6) and (10), we can write

$$P_x = \frac{P_y}{(1 + HK^4/D)^2}, \tag{15}$$

which is

$$\approx \frac{P_v s^2/\sigma^2}{(1 + HK^4/D)^2}$$

because of (14).

It remains to find a relation between s^2/σ^2 and the (mean) lateral pressure which determines the extent of the contact. In the limit in which the fiber is stiff, as indicated in Fig. 2a, we have approximately $\langle f \rangle \approx D\langle y \rangle$, since $\langle u \rangle \approx \langle y \rangle$ in (4). The mean force $\langle f \rangle$ per unit length is, of course, the (linear) pressure we are interested in. To express (13) as a function of $\langle y \rangle$ only, we must eliminate t from (11) and (12). The result of this calculation is presented in approximate form:

$$\frac{s^2}{\sigma^2} = \left(1 + \frac{\pi^2}{4}\frac{\sigma^4}{\langle y \rangle^4}\right)^{-\frac{1}{2}}. \tag{16}$$

If the fiber cannot be assumed as stiff, the situation of Fig. 2b applies. We find that the surface deformation is more correctly given by the function

$$u(z) = \begin{cases} v(z) - x & v \geqq x + t \\ 0 & v < x + t \end{cases} \tag{17}$$

and that the mean of (17), rather than $\langle y \rangle$, determines the lateral pressure. The statistics of (17) are difficult to evaluate, since v and x are interrelated as a result of (15). According to (15), $x(z)$ essentially comprises all Fourier components of $v(z)$ having wave numbers $K < (D/H)^{\frac{1}{4}}$. As is evident from Fig. 2b, it is the remaining spectrum with $K > (D/H)^{\frac{1}{4}}$ that contributes to $u(z)$ of (17). This fact is the basis for the following estimate for the mean of (17):

$$\langle u \rangle^2 = \frac{\langle y \rangle^2}{s^2} \int_{(D/H)^{\frac{1}{4}}}^{\infty} P_v dK$$

$$\approx \frac{\langle y \rangle^2}{\sigma^2} \int_{(D/H)^{\frac{1}{4}}}^{\infty} P_v dK. \tag{18}$$

If the mean lateral pressure is $f_0 = \langle f \rangle$, we can write with (4), (16), and (18)

$$\frac{s^2}{\sigma^2} = \left[1 + \frac{\pi^2}{4}\frac{D^4}{f_0^4}\left(\int_{(D/H)^{\frac{1}{4}}}^{\infty} P_v dK\right)^2\right]^{-\frac{1}{2}}. \tag{19}$$

This relation together with (15) permits us to calculate the spectral

density P_x of the fiber deformation, if the spectrum of v and the mean pressure f_0 are known.

IV. DISTORTION LOSS

A significant exchange of power between two modes in a multimode fiber occurs when a periodic disturbance exists whose wave number K equals the phase lag between the two modes. This phase lag is in general a complicated function of the mode numbers involved and of the refractive index profile across the fiber core. Only if the index decreases as the square of the fiber radius (parabolic profile) is the phase lag the same for all modes coupled. This phase lag is

$$K_c = \frac{(2\Delta)^{\frac{1}{2}}}{a_c}, \tag{20}$$

when a_c is the core radius and Δ the relative index difference between core axis and cladding. If the index is uniform within the core and decreases abruptly to the cladding value (step-index profile), the coupled mode pairs have typically a smaller phase lag than K_c, although the phase lag approaches K_c for modes close to cutoff. For this profile, it is the spectral density $P_x(K)$ in the regime $0 < K \leqq K_c$, which determines coupling and coupling loss.

Equation (15) relates P_x to the spectral density P_v, which characterizes the original source of disturbance. We know little about its character; thus, to cover a broad variety of possibilities, we use the rather general functional description

$$P_v = \frac{P_v(0)}{(1 + l^2K^2)^\mu}, \tag{21}$$

with $\mu > 1$ and l large compared to $1/K_c$ and $(H/D)^{\frac{1}{2}}$. This stipulates a decrease of $P_v(K)$ in the vicinity of K_c in agreement with available experimental evidence.[2] The parameter l has the physical significance of a correlation distance. Integration of (21) yields a relation between $P_v(0)$ and the standard deviation σ introduced earlier:

$$P_v(0) = \frac{2\Gamma(\mu)\sigma^2 l}{\Gamma(\frac{1}{2})\Gamma(\mu - \frac{1}{2})}; \quad \mu > 1. \tag{22}$$

Coupling among neighboring modes dominates the power transfer inside the fiber. In the limit of very large mode numbers, the resulting power flow can be modeled by a diffusion process.[8] More specifically, if one defines a (continuous) mode variable r, one finds the power $\phi(r)$ in a mode group characterized by r from diffusion equations of

the form[8,9]

$$\frac{d}{dr}\left[\frac{K_c^4}{8\Delta} r^4 P_x(rK_c)\frac{d\phi}{dr}\right] + \gamma\phi = 0 \tag{23}$$

for the step profile and

$$\frac{d}{dr}\left[\frac{K_c^4}{4\Delta} r P_x(K_c)\frac{d\phi}{dr}\right] + \gamma\phi = 0 \tag{24}$$

for the parabolic profile. The term $\gamma\phi$ accounts for an overall decay of ϕ as a result of coupling loss. This excess loss is caused by radiation from modes at or beyond cutoff ($r \geqq 1$). The mathematical model considers the steeply rising loss at $r > 1$ to first approximation by the boundary condition $\phi(1) = 0$. In addition, we have $d\phi/dr = 0$ at $r = 0$, since no power can be lost at $r = 0$.

Equation (24) has an infinite set of eigensolutions[8] for arbitrary P_x; such solutions also exist for (23) at least if $\mu > 1$ and $l > 1/K_c$. In any of these cases, the lowest eigenvalue γ_0 is also the smallest and denotes the loss value approached asymptotically by long fibers once a "steady state" is reached. In the case of (24), γ_0 can be computed rigorously for arbitrary P_x; a way of finding a good upper limit for γ_0 of (23) is outlined in the appendix. The result is

$$\gamma_0 \leqq \frac{4\mu - 3}{16}\frac{K_c^4}{\Delta}\frac{P_y(K_c)}{1 + \dfrac{4\mu - 3}{4\mu + 13}(HK_c^4/D)^2} \tag{25}$$

for the step profile and

$$\gamma_0 = 0.36\,\frac{K_c^4}{\Delta}\frac{P_y(K_c)}{(1 + HK_c^4/D)^2} \tag{26}$$

for the paraholic profile, with

$$P_y(K_c) = \frac{2\Gamma(\mu)\sigma^2 l}{\Gamma(\frac{1}{2})\Gamma(\mu - \frac{1}{2})(lK_c)^{2\mu}} \times\left(1 + \frac{\pi\Gamma^2(\mu)\sigma^4 H^{\mu-\frac{1}{2}}}{(2\mu - 1)^2\Gamma^2(\mu - \frac{1}{2}) f_0^4 l^{4\mu-2} D^{\mu-9/2}}\right)^{-\frac{1}{4}} \tag{27}$$

from (19) and (22). Note that (25) is an upper limit and that these derivations are subject to the limitation $\mu > 1$ and that l must be large compared to $1/K_c$ and $(H/D)^{\frac{1}{4}}$.

In general, it will be necessary to determine the parameters in (21) from experimental evidence. For the numerical results following in the next sections, we have used $\mu = 3$ as a typical and realistic example.[2]

In this case, the use of (20) and (27) converts (25) and (26) into

$$\gamma_0 \leqq \frac{3}{2\pi} \frac{\sigma^2 a_c^2}{l^5 \Delta^2} \frac{1}{\left(1 + \frac{144\Delta^4 H^2}{25 a_c^8 D^2}\right)\left(1 + \frac{64\sigma^4 H^4 D^4}{225 f_0^4 l^{10}}\right)^{\frac{1}{4}}} \tag{28}$$

for the step profile and

$$\gamma_0 = \frac{96}{25\pi} \frac{\sigma^2 a_c^2}{l^5 \Delta^2} \frac{1}{\left(1 + \frac{4\Delta^2 H}{a_c^4 D}\right)^2 \left(1 + \frac{64\sigma^4 H^4 D^4}{225 f_0^4 l^{10}}\right)^{\frac{1}{4}}} \tag{29}$$

for the paraholic profile.

V. FIBER STORAGE DRUM

The main ohjective of this theory is, of course, the design of jackets that protect the fiher from distortion and the loss associated with it; hut, to hegin with a simple prohlem, let us first ask how the loss increases in a fiher when it is wound on a drum. Clearly, the drum surface properties and the winding force are important factors. We assume the radius ρ of the drum to he so large that the constant curvature of the fiher has no noticeahle influence on the loss. If we apply a tensile force F, the fiher presses against the drum surface with a (linear) pressure

$$f_o = F/\rho. \tag{30}$$

With these definitions, the distortion loss as a result of the winding pressure can he directly computed from (25) and (26). The results are illustrated by the following representative example:

(*i*) Fiher characteristics:
Core radius $a_c = 40$ μm.
Outside radius $a_1 = 60$ μm.
Relative index diffcrence $\Delta = 0.005$.
Young's modulus (silica) $E_1 = 7000$ kg/mm^2 (10^7 psi).

(*ii*) Drum surface statistics:
Standard deviation $\sigma = 1$ μm.
Correlation length $l = 1$ mm.
Spectral coefficient $\mu = 3$.

The evaluation of (25) and (26) for $\mu = 3$ is given in (28) and (29). We discuss only the step-index profile in the following. The results for the paraholic profile can he obtained from (29); they differ little from those of the step profile.

Figure 3 is an evaluation of (28) as a function of Young's modulus of the drum surface material with the pressure f_o as a parameter. The

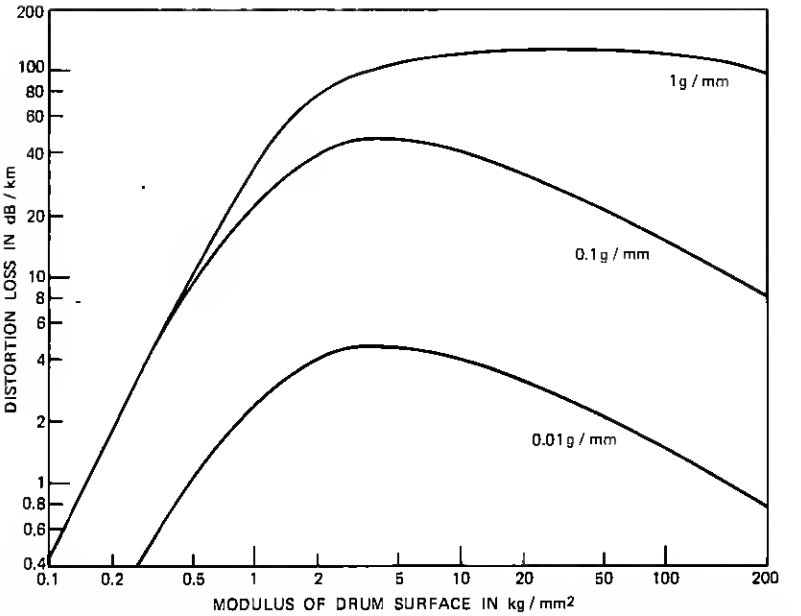

Fig. 3—Distortion loss versus drum surface modulus according to eq. (30); fiber diameter is 120 μm, core diameter is 80 μm, relative index difference is 0.5 percent, rms drum surface roughness is 1 μm, correlation distance is 1 mm. Mean lateral force per unit length is the parameter.

plot represents the loss for drums of different elasticity provided that the surface statistics are the same for all. If $F = 100$ g and $\rho = 10$ cm ($f_o = 1$ g/mm), the distortion loss can he as high as 130 dB/km. For low pressures, the loss decreases with increasing rigidity of the drum surface, as the fiher ceases to conform to the irregularities of the surface. If the drum is soft, the loss is reduced independently of the pressure, since the fiher sinks into the surface and smoothes the irregularities. Thus, hoth hard and soft surfaces have a tendency to decrease the excess loss for a given pressure. The effect of a hard surface, however, strongly depends on the pressure applied. A reduction of the loss to 0.5 dB/km independently of pressure requires an extremely soft surface (0.11 kg/mm^2 = 157 psi) for the kind of fihers characterized hy this example. Typical winding forces which are caused hy the pulling operation itself or applied in rewinding operations are in the range hetween 10 to 100 g. Thus, a loss increase of 100 dB/km or more as a result of drum storage is not surprising.

Equation (28) shows that γ_0 is proportional to Δ^{-6} in the case of "soft" surface conditions, i.e., when the first parenthesis in the denominator of (28) is much larger than unity. Hence, an increase in the

index difference hy a factor of 1.5 would reduce the loss coefficient in this range hy one order of magnitude. Of course, these results depend on the surface statistics assumed here. For arhitrary μ, the excess loss coefficient is proportional to $\Delta^{1-\mu}$ if the surface is hard and to $\Delta^{-3-\mu}$ if the surface is soft.

Next, let us consider a jacketed fiber wound onto a slightly rough drum. The lateral rigidity D_2 of the jacket is, in general, different from the rigidity D_1 of the drum surface. To account for the compressihility of hoth, one must use an effective rigidity

$$D_e = \frac{1}{1/D_1 + 1/D_2} \tag{31}$$

in (25) to (29). There will he statistical variations of the jacket thickness and these are likely to differ from those of the drum surface. If one or the other dominates and follows the characteristics (21) with $\mu = 3$, one can still use (28) or (29) or Fig. 4 to determine the distortion loss if one incorporates (31).

VI. PLASTIC JACKET DESIGN

In a cable, the fihers will he organized in hundles and pressed together hy binding or sheathing forces, by cahle deformations, and hy pressure on the cable, once it has been placed.

Considering only one cross-sectional dimension, we assume a typical fiher of the hundle to he contacted by two others, one on either side. All fihers have plastic jackets, so that elastic surfaces of equal modulus press against each other. The situation is similar to that described by (31) except that now D_1 and D_2 of that equation are identical and equal to the modulus (or the rigidity D) of the jacket material. Hence, $D_e = D/2$. Other differences with respect to the previous model are the two lines of variable pressure and a total of four random variahles involved in the deformation of the fiber. These variahles are the jacket thickness variations v_1 and v_2 of the fiher in the middle and the variations v_3 and v_4 referring to the jackets on the outside. If we assume again complete and continuous contact, the resulting differential equation hecomes

$$2\frac{H}{D}\frac{d^4x}{dz^4} + 2x = v_1 - v_2 - v_3 + v_4, \tag{32}$$

where the relation $D_e = D/2$ has heen used. The variables v_1 to v_4 are statistically independent, hut they are samples of the same ensemble. Therefore, they all have the same spectral density $P_v(K)$ and the spectral density of the sum on the right of (32) is 4 $P_v(K)$. After Fourier transformation and the insertion of spectral densities into (32),

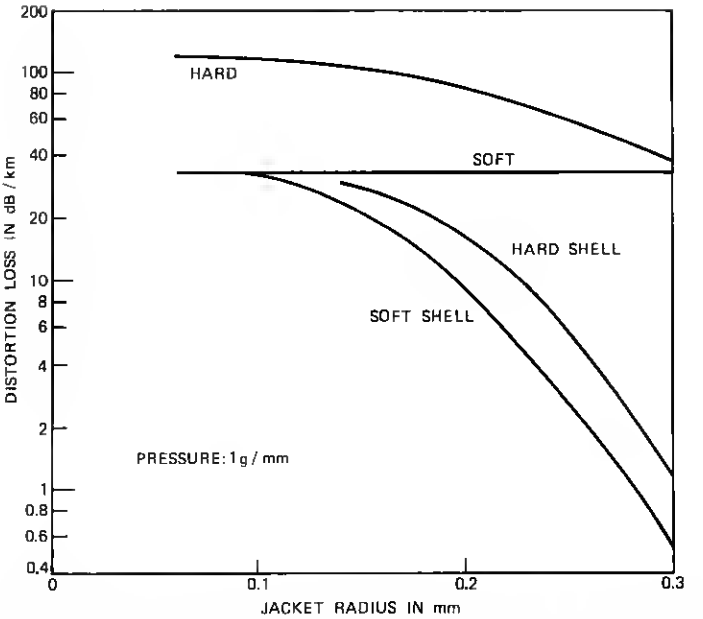

Fig. 4—Distortion loss versus outside jacket radius according to eq. (30); fiber characteristics as in Fig. 3, rms jacket thickness variation 1 μm, correlation distance 1 mm, mean lateral pressure 1 g/mm. Curves refer to four jacket configurations listed in Table I.

all numerical factors cancel, leaving us with the mathematical relationships derived earlier. As a result, (28) and (29) are also applicable to the problem of the jacketed fiber in a bundle, provided that the statistics of the jacket thickness variations can be described by (21) with $\mu = 3$. Now D stands for the modulus of the jacket and H for the combined stiffness of fiber and jacket. The stiffness of the latter is

$$H_2 = \frac{\pi}{4} E_2(a_2^4 - a_1^4) \tag{33}$$

with E_2 being Young's modulus of the jacket material and a_2 and a_1 its outer and inner radius, respectively. In the case of several jackets, H is generally the sum over all stiffnesses. If the outer jacket is the softer one and sufficiently thick that a deformation beyond its elastic limit is unlikely, D is simply the modulus of the outer jacket. If the outer jacket is harder than the inner one and has a thickness b small compared to its outer radius a_2, we have[10]

$$D \approx E_2 + E_3 \frac{b^3}{a_2^3}, \tag{34}$$

where E_2 and E_3 are the moduli of the inner and the outer jacket, re-

spectively. If the inner jacket is very soft and thick, we must consider the hard outer shell and the fiber as two independent systems, each undergoing deformations governed by differential equations similar to (32). The result are four instead of two expressions in the denominator of (28) and (29), one pair comprising the H and D parameters of a hard shell surrounding a soft material, and the other pair comprising the H and D parameters of a fiber imbedded in a soft material.

The following is a discussion of four alternative jacket configurations. As a realistic example, we consider the same fiber characteristics and the same statistical parameters listed in the previous section for the drum surface. Table I gives a description of the jackets. The first is made entirely from a soft plastic, the second from a hard plastic, and the third and fourth are hybrid structures. We assume a modulus of 1 kg/mm² (1400 psi) for a typical soft material and 100 kg/mm² for a typical hard material. In Figs. 4 and 5, the outer jacket radius a_2 is plotted versus the excess loss computed for each structure if the mean lateral pressure is either 1 g/mm (Fig. 4) or 0.1 g/mm (Fig. 5). The pressure obviously determines the choice between a soft or a hard material, if the jacket is to be made from one material alone. The decrease of the loss contribution with increasing jacket radius in case of the hard jacket comes about as a result of the increase in stiffness. The corresponding increase afforded by the soft jacket is negligible. The last two columns of Table I list the D and H parameters used in each case.

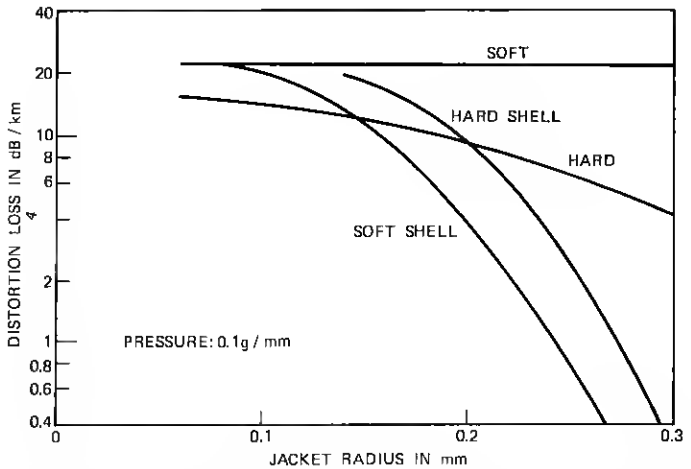

Fig. 5—Distortion loss versus outside-jacket radius according to eq. (30); fiber characteristics as in Figs. 3 and 4, jacket statistics as in Fig. 4, and mean lateral pressure 0.1 g/mm. Curves refer to four jacket configurations listed in Table I.

Table I — Characteristics of several types of protective jackets for optical fibers

	Modulus in kg/mm²	Inside Radius in mm	Outside Radius in mm	Rigidity in kg/mm²	Stiffness in kg mm²
Soft Jacket	1	0.06	a_2	1	0.0713
Hard Jacket	100	0.06	a_2	100	$0.0702 + 78.5a_2^4$
Inside Jacket	100	0.06	$a_2 - 0.02$	1	$0.0702 + 78.5(a_2 - 0.02)^4$
Outside Jacket	1	$a_2 - 0.02$	a_2		
Inside Jacket	1	0.06	$a_2 - 0.04$	1	0.0713
Outside Jacket	100	$a_2 - 0.04$	a_2	$1 + \frac{0.0064}{a_2^3}$	$78.5a_2^4 - 78.5(a_2 - 0.04)^4$

The third structure has a hard jacket padded with a soft outer layer. The layer thickness of 20 μm was cbosen to avoid any deformation beyond its elastic limit. Tbe fourth structure bas a hard shell surrounding a soft material. Tbe thickness of this sbell should be approximately 0.02 a_2. This optimum is a result of an increase botb in stiffness and lateral rigidity as the shell tbickness is increased, so that the retention lengtb R, whicb is the ratio of the two, passes througb a maximum. To simplify matters, we have cbosen a thickness of 40 μm independent of tbe sbell radius. Tbe two pairs of D-H values listed in tbe case of tbe fourtb configuration refer to tbe two independently deforming structures (shell and fiber) which must be considered in this case, as was mentioned earlier. The slight advantage of the soft over the hard shell, evident in Figs. 4 and 5, is too small to he decisive. It may well be offset by weight and cost considerations. Tbe substantially improved fiber protection afforded by tbe hybrid structures as compared to simple jackets, bowever, is well wortb considering. A jacket diameter of 0.5 to 0.6 mm permits a virtual elimination of the distortion loss in case of the example considered here. A similar reduction by a single hard jacket requires at least twice this jacket diameter.

The excess loss computed for tbe structure with a hard shell vanishes wben the modulus of the inner jacket is reduced to zero. This implies tbat the protection provided hy a stiff shell that surrounds tbe fiber in a loose way witbout any material in hetween is perfect. Of course, this would indeed be true if tbe only forces present were lateral outside forces borne by the shell. In practice, tbere are other forces not considered bere; forces tbat press the fiber against tbe inside jacket wall in a cable bend, for example. Sucb forces determine the distortion loss of the loosely jacketed fiber. Altbougb this is an important problem to consider, it is beyond the scope of this work.

Properties similar to those of byhrid jackets can also be obtained with reinforced jackets. The reinforcement could, for example, consist of strong fine fihers running parallel or sligbtly stranded to the optical fiber imbedded in a relatively soft jacket material. The fiber material could be plastic, glass, or graphite, tbe latter being particularly suited because of its low weigbt, higb tensile modulus, and higb strengtb. Also, as graphite fiber is available with diameters down to 5 μm, its incorporation into tbe jacket sbould be manageable without causing permanent internal stresses resulting in distortion loss by itself. The advantage of tbe reinforced jacket is its anisotropy which combines stiffness with lateral compressibility. Althougb tbese properties are difficult to compute, an estimated loss reduction of two orders of magnitude for a jacket 0.4 mm in diameter seems achievable with the fiber cbaracteristics listed in the previous section.

The effect of the reinforced jacket and of the configurations 1, 3, and 4 in Tahle I is a comhination of stiffness and compressihility, while that of configuration 2 is hased on stiffness alone, preventing its conformance to surface irregularities. Mathematically, these two effects are distinguished hy the two parentheses in the denominator of (25) or (26). It is important to note that the first parenthesis depends strongly on the fiber characteristics. An effective jacket implies $HK_c^4/D \gg 1$ in (25), so that the loss reduction afforded hy the first group of jackets is proportional to K_c^8 or, with (20), to Δ^4/a_c^8. As a result, a small increase in index difference suhstantially increases the effectiveness of these jackets. If, for example, $\Delta = 2$ percent instead of 0.5 percent as previously assumed, the soft jacket, the reinforced jacket, and the two hyhrid structures reduce the excess loss coefficient hy an additional factor of 256, while the effect of the hard jacket remains the same. This strongly emphasizes the importance of this first group of jackets and the need for fihers with large index difference.

Of course, the ahove dependence on Δ holds only as long as the predominant sources of loss are indeed those assumed here. If other sources of loss dominate, as, for example, the influence of a very lossy cladding material, typically only a fraction of all trapped modes propagates in the steady state. In this case, Δ in (20) and in the ahove arguments must he replaced hy $N^2/2n$, where N is the effective numerical aperture characterizing the mode distrihution of the steady state and n the refractive index of the core.

VII. CONCLUSIONS

Optical fihers need protection from lateral forces and this requires a careful design of the fiher jacket. The jacket should have a high flexural rigidity or stiffness in comhination with a good lateral compressihility. These properties define a retention length within which the jacket essentially ahsorhs irregularities impressed from the outside. Longer irregularities deform the fiher and can lead to distortion loss if they comprise spectral components in the vicinity of the critical wave numher of the fiher.

Although the forces to which a fiher is suhjected in a cahle are difficult to estimate, one gains a fair notion of the sensitivity of the fiher to such forces hy winding it on a drum with minute surface irregularities. This can hest he illustrated hy way of a representative example. Consider a silica fiher, 120 μm in diameter, that has a relative index difference of $\Delta = 0.5$ percent and a core diameter of 80 μm. Assume a tensile force of hetween 10 and 100 g applied when winding the fiher on a drum, which has a diameter of 10 cm and an rms surface roughness of 1 μm. The estimated loss increase is hetween 50 and 130 dB/km

depending on the winding force applied. A winding force of 10 g corresponds to a mean pressure of 0.1 g/mm on tbe fiber.

Now consider five types of jackets:

(*i*) A soft plastic jacket baving a modulus of 1 kg/mm^2.
(*ii*) A jacket of bard plastic witb 100 kg/mm^2.
(*iii*) The same as (*ii*) padded with a thin layer of the material used in (*i*).
(*iv*) A sbell of the material of (*ii*) on top of soft material as used in (*i*).
(*v*) A soft jacket reinforced by a filler of strong plastic, glass, or graphite fiber.

We find tbat, for equal jacket diameters, (*i*) is almost always better tban (*ii*) except when Δ and the lateral forces are small. For tbe fiber of the previous example, the jacket (*i*) reduces the excess loss cofficient hy a factor of 3. If optimized in thickness, the sbell (*iv*) is about as useful as (*iii*). An overall tbickness of 0.6 mm permits in both cases a reduction of the loss coefficient by two orders of magnitude. A graphite reinforced jacket of equal size sbould have at least the same effect.

Tbe effectiveness of a jacket is a strong function of tbe fiber to be protected. For example, the factor by which the jacket reduces the loss coefficient is proportional to Δ^4. In addition, the distortion loss of tbe unprotected fiber is a function of Δ. Hence, tbe loss coefficient may typically scale as Δ^{-2} for a fiher witbout jacket, but as Δ^{-6} for the jacketed fiber. In other words, if the index difference in tbe previous example bad been 1 percent instead of 0.5 percent, the excess loss would have heen initially less than 35 dB/km on the drum and 0.5 dB/km after protection with a simple soft jacket. Cable forces are likely to be stronger and less uniform than those encountered on a storage drum and may necessitate a fiber protection hy the more expensive hybrid jackets or even by reinforcement.

VIII. ACKNOWLEDGMENTS

Helpful discussions with E. A. J. Marcatili, W. B. Gardner, and L. L. Blyler are gratefully acknowledged.

APPENDIX

Rayleigh-Ritz Limit for Steady-State Loss

The Rayleigb-Ritz metbod[12] provides a surprisingly close upper limit for the lowest eigenvalue of differential equations of tbe type in (25) or (26) if a reasonable trial solution for tbe lowest eigenvalue can be constructed. We demonstrate this for an important subclass of (25).

Consider the case that l in (23) is very large and $(H/D)^{\frac{1}{2}}$ in (17) is very small compared to $1/K_c$, so that $P_x \approx P_y \approx 2\Gamma(\mu)\sigma^2 l/\Gamma(\frac{1}{2})\Gamma(\mu - \frac{1}{2})(lK)^{2\mu}$. After suitable normalization, (25) is then of the form

$$\frac{d}{dr}\, c(r)\, \frac{d\phi}{dr} + g\phi = 0 \quad \text{with } c = r^{-\sigma} \tag{35}$$

and $\sigma > -2$. Multiply (36) by ϕ, integrate over r from 0 to 1, and solve for g. With the boundary condition $\phi(1) = 0$, one arrives at

$$g = \frac{\int_0^1 c \left(\frac{d\phi}{dr}\right)^2 dr}{\int_0^1 \phi^2 dr}. \tag{36}$$

We choose the trial solution

$$\phi = 1 - r^{\nu} \quad \text{with } \nu > 1, \tag{37}$$

so that the boundary condition $d\phi/dr = 0$ at $r = 0$ is also satisfied. We insert (37) into (36) to obtain

$$g = \frac{1}{2}\, \frac{(2\nu + 1)(\nu + 1)}{2\nu - \sigma - 1}. \tag{38}$$

Since (38) is larger than the true eigenvalue γ_0 for all ν, we find the best approximation from $dg/d\nu = 0$. The result is

$$\nu = \frac{1}{2}\left[(\sigma + 1) + (\sigma^2 + 5\sigma + 6)^{\frac{1}{2}}\right] \approx \sigma + \frac{7}{4} \tag{39}$$

and

$$g \approx \sigma + \frac{10}{4}. \tag{40}$$

The quality of this result can be checked against the rigorous solution $\gamma_0 = \pi^2/4 = 2.467$ as compared to $g = 2.5$ for $\sigma = 0$. One can show that (40) converges on γ_0 for increasing σ. For $\sigma < 0$, (40) proves useful even beyond the regime of validity of the trial solution. For $\sigma = -1$, for example, the rigorous solution is[8] $\gamma_0 = 1.446$, while (40) yields $g = 1.5$. This case, by the way, is the solution of (26).

The trial solution (37) is useful also in the case that P_x of (24) has the more general form given by (17) and (22), but it becomes substantially more difficult to optimize ν. One can convince oneself that the final result (27) converges on the form derived in (40) in the limits $(D/H)^{\frac{1}{2}} \gg K_c$ and $(D/H)^{\frac{1}{2}} \ll K_c$.

REFERENCES

1. R. D. Maurer, private communication, 1972.
2. W. B. Gardner, "Microbending Loss in Optical Fibers," B.S.T.J., this issue, pp. 457.
3. W. A. Gambling, D. N. Payne, and H. Matsumura, "Gigahertz Bandwidths in Multimode, Liquid-Core, Optical Fiber Waveguide," Optics Communications *6*, No. 4 (December 1972), pp. 317–322.
4. D. B. Keck, "Observation of Externally Controlled Mode Coupling in Optical Waveguides," Proc. IEEE, *62*, No. 5 (May 1974), pp. 649–650.
5. L. G. Cohen and D. Gloge, "Mode Delay in Selfoc Fibers of the New Type," unpublished work.
6. D. Marcuse, "Pulse Propagation in Multimode Dielectric Waveguides," B.S.T.J., *51*, No. 7 (July–August 1972), pp. 1199–1232.
7. L. A. Galin, *Contact Problems in the Theory of Elasticity*. Edited by I. N. Sneddon. Translated by Mrs. H. Moss. Raleigh, N.C.: North Carolina State College, 1961.
8. R. Deutsch, *Nonlinear Transformations of Random Processes*, Englewood Cliffs, N.J.: Prentice-Hall, 1962, pp. 15–26.
9. D. Gloge, "Optical Power Flow in Multimode Fibers," B.S.T.J., *51*, No. 8 (October 1972), pp. 1767–1783.
10. D. Marcuse, "Losses and Impulse Response of a Parabolic Index Fiber with Random Bends," B.S.T.J., *52*, No. 8 (October 1973), pp. 1423–1437.
11. S. Timoshenko and S. Woinowsky-Krieger, *Theory of Plates and Shells*, New York: McGraw-Hill, 1959.
12. P. M. Morse and H. Feshbach, *Methods of Theoretical Physics, II*, New York: McGraw-Hill, 1953, p. 1115.